buildings

Article

Evaluation of Ultra-High-Performance Concrete Columns at High Temperatures after 180 Days of Curing

Roberto Christ [1,*], Lucas Rafael Lerner [2], Hinoel Z. Ehrenbring [2], Fernanda Pacheco [2], Fabricio L. Bolina [3], Giovana Poleto [2], Augusto Masiero Gil [4] and Bernardo F. Tutikian [2]

1 Civil and Environmental Department, Universidad de la Costa, Calle 58 #55-66, Barranquilla 080002, Colombia
2 Polytechnical School, University of Vale do Rio dos Sinos—UNISINOS, São Leopoldo 93040-230, Brazil; lucaaslerner@gmail.com (L.R.L.); hzamis@unisinos.br (H.Z.E.); fernandapache@unisinos.br (F.P.); giovanapoleto@hotmail.com (G.P.); bftutikian@unisinos.br (B.F.T.)
3 Structures and Civil Construction Department, Federal University of Santa Maria (UFSM), Santa Maria 97105-900, Brazil; fabricio.bolina@ufsm.br
4 Department of Civil and Environmental Engineering, Michigan State University—Spartans Will, Springfield, MI 48824, USA; augusto.masiero@hotmail.com
* Correspondence: rchrist@unisinos.br

Abstract: Ultra-high-performance concrete (UHPC) is a material that has high compactness, low porosity, and high mechanical strength, with especially high tensile strength. Due to these characteristics, the behavior of the material when exposed to high temperatures is debatable. The high amount of fibers in the mixture, which makes UHPC present a high tensile strength, is seen as one of the arguments for the good performance of the material when exposed to high temperatures. The objective of this study was to evaluate the behaviors of ultra-high-performance concrete columns with hybrid steel and polypropylene fibers and no loose reinforcements when subjected to elevated temperatures after 180 days of curing. The exposure of concrete with a low age, less than 90 days, to high temperatures results in greater damage to the concrete due to spalling, and because of this, this study sought to evaluate the UHPC with a higher age. Two columns were manufactured with a cross-section of 250 mm × 250 mm and a height of 2800 mm. A heating regime followed the heating curve of standard ISO 834-1. The physical characteristics of the samples were evaluated during and after exposure to high temperatures with measurements of the decreases in the cross-section and surface aspect. Effects on the compressive strength, modulus of elasticity, and apparent density were evaluated with cylindrical test bodies of 100 mm in diameter and 200 mm in height. These samples were cured for 180 days, subjected to the same heating regime, and evaluated after cooling. The results showed an increase in the compressive strength with an increasing temperature up to a factor of 30% at a temperature of 400 °C. The modulus of elasticity and apparent density decreased gradually as the temperature increased, with maximum decreases of 29% and 6%, respectively. Throughout heating, audible cracks were heard from the columns because of spalling. The spalling frequency peaked at an oven temperature of 600 °C, and testing was suspended at 78 min after the complete rupture of a column section. On average, 46.5% of the column cross-sections suffered from spalling.

Keywords: ultra-high performance concrete; high temperature; columns; steel fiber; curing concrete

check for updates

Citation: Christ, R.; Lerner, L.R.; Ehrenbring, H.Z.; Pacheco, F.; Bolina, F.L.; Poleto, G.; Gil, A.M.; Tutikian, B.F. Evaluation of Ultra-High-Performance Concrete Columns at High Temperatures after 180 Days of Curing. *Buildings* **2023**, *13*, 2254. https://doi.org/10.3390/buildings13092254

Academic Editors: Binsheng (Ben) Zhang and Wei (David) Dong

Received: 26 May 2023
Revised: 21 August 2023
Accepted: 23 August 2023
Published: 5 September 2023

1. Introduction

The definition of ultra-high-performance concrete (UHPC) varies with international standards, but common characteristics are a ductile compound with elevated mechanical resistance, post-fissuring tensile strength, and durability [1,2]. The minimal compression strength varies between 120 MPa and 150 MPa, as per the standard [1,3–5].

The mechanical performance and durability of UHPC are related to the aggregate packing of the materials, a low water/agglomerate ratio, and the use of low-granulometry supplementary cementitious materials, such as silica fume [6–8]. Granular packing allows an UHPC to have low porosity, which is important when concrete is subjected to elevated temperatures [9,10]. Due to the low porosity and perfect granular packing, the physical and chemical effects of UHPC, when exposed to high temperatures, are not well known. Coarse aggregates are not commonly found in UHPC, and their absence prevents the formation of a weak transition zone between cement and aggregates and yields desired mechanical resistance and durability levels [8].

Concrete exposed to elevated temperatures underwent physical and chemical changes that decreased the compressive strength. These changes were related to the characteristics of the compound, such as the water/cement ratio, internal humidity level, type of cement, and aggregates [11]. Xiong et al. [12] denoted two residual mechanical properties of importance to UHPC following exposure to high temperatures: compression strength and the modulus of elasticity. Other physical properties of interest were the thermal conductivity, specific heat, and density.

Besides decreases in compressive strength, another phenomenon observed in concretes exposed to elevated temperatures was spalling or the breaking away of layers of the structural element. This phenomenon was caused by water-induced expansion inside the concrete upon heating and an increased internal pressure [13]. Aggregate expansion, which occurred at elevated temperatures, also contributed to spalling depending on the type of aggregate [11]. Quartz begins to have its expansion altered at a temperature of 400 °C, different from other materials, such as basalt and limestone, among others. The effect of some aggregates might be higher than the type or amount of cement used in the compound. Other physical and chemical changes could result in additional damages and a loss of performance [14].

The addition of synthetic fibers could be an alternative technique to decrease UHPC internal stresses due to water vapor pressure and resist spalling [15,16]. Some studies evaluated the addition of between 2 kg/m^3 and 3 kg/m^3 of polypropylene fibers in UHPC to determine their effect on spalling [15–17], while Sanchayan and Foster [18] made use of up to 6.5 kg/m^3 of polyvinyl alcohol (PVA) fibers. Choe et al. [19] determined that adding 0.15%, by volume, of synthetic fibers completely prevented spalling in UHPC, while Zheng et al. [20] achieved the same result with a 2.73 kg/m^3 content. Overall, while there was no consensus on the ideal amount of polymer fibers, there was evidence that their disintegration decreased pore pressure effects and spalling.

If coarse aggregates were not used, the resulting matrix was more compacted, and tiny pores could significantly relieve water steam pressure. Furthermore, the expansion of metallic fibers could also contribute to this result. Li et al. [21] noted that heated metallic microfibers tended to lose adhesiveness with the UHPC matrix and cause damage to the structural element. However, Gravit and Golub [22] reported that even though metallic fibers had higher melting points than polymer fibers, they could still contribute to spalling mitigation in hybrid compounds.

Two or more types of sand with varying granulometry can improve packing in UHPC. Sands were usually quartz-based and corresponded to 40% to 60% of the volume of the mixture [2]. The phase change of quartz started at temperatures between 500 °C and 600 °C, and elevated expansion occurred between 600 °C and 1000 °C [14]. This phase change causes the material to have a significant increase in volume. Since the UHPC matrix is of high density, this increase in volume causes internal tensile stresses to occur, thus increasing the occurrence of spalling.

The mechanical properties of concrete, such as the compression strength and modulus of elasticity, were affected by elevated temperatures. These changes take place up to a certain temperature, provisionally 400 °C; up to this temperature, the anhydrous cement that still exists in the mix binds with the water that moves via the effects of internal thermals, and thus, the resistance is improved. It is necessary to understand that concrete does not remain at this temperature for a long time, because if this occurs, the chemical bond will not occur, and it takes time for this bond to occur. However, since concrete has low thermal conductivity, only the exposed surface tends to be involved [23]. Abid et al. [24] noted that several experimental studies used test bodies to evaluate UHPC properties. In general, it was concluded that the loss of UHPC mechanical strength was related to the type of aggregate, heating rate, cooling rate, test body size, and compression strength of concrete [12]. However, Kodur et al. [25] noted that most studies evaluated UHPC performance solely through test bodies. This agreed with Gil et al. [26], which denoted that an analysis of cylindrical test bodies was essential, but insufficient, to fully assess the behavior of the mixture in realistic structural elements.

Considering that real size tests are needed and there is a lack of research in this area, the objective of this study was to evaluate the performance of UHPC columns reinforced with polymer and steel fibers in samples with realistic physical scales, cured for 180 days and subjected to a standard heating curve. Only a few laboratories count with this type of oven and can perform those tests. This is the reason why this paper is innovative and contributes to an understanding of fire in UHPC materials. The curing period was chosen to approximate the actual conditions that might be encountered, since the probability of a structure burning at early ages is low. Despite that, a study showed that until 180 days, there is a relevant humidity variation on the concrete surface, and thus, this time is recommended [27]. Losses in the compression strength and modulus of elasticity were evaluated as well.

2. Materials and Methods

The UHPC used in this study [1] is shown in Table 1.

Table 1. UHPC mix ratio.

Materials	kg/m^3
Portland cement	490
Silica fume	269
Fly ash	235
Quartz sand	1025.5
Water	179
Superplasticizer additive	17.6
Steel fibers	120
PVA fibers	6

The cement used in the mixture was Portland cement CEM II 40, containing 20.90% SiO_2, 3.64% Al_2O_3, 63.68% CaO, and 3.03% SO_3. The specific density of cement was 3.10 g/cm^3, and the Blaine surface area was 4.989 cm^2/g. The silica fume had a silicon content of 88.43% and a specific mass of 2.35 g/cm^3. The fly ash had a silicon content higher than 50% and a specific mass of 2.10 g/cm^3. Quartz sand was sourced from a river and, following washing and drying, had a specific mass of 2.66 g/cm^3. Figure 1 presents the granulometric distribution curves of the materials.

Reinforcement of the column test bodies consisted of hybrid fibers with a total content of 2%, concerning the volume of concrete, and no loose reinforcements. More specifically, the fiber content consisted of 1.6% steel fibers and 0.4% PVA fibers. Fiber types are shown in Figure 2. The steel fibers were 25 mm in length and 0.75 mm in diameter with a tensile strength of 1100 MPa and an aspect ratio of 33. The modulus of elasticity of the steel fibers was 210 GPa. The PVA fibers were 12 mm in length and 0.04 mm in diameter with a tensile strength of 1600 MPa and an aspect ratio of 300. The modulus of elasticity of PVA fibers was 41 GPa.

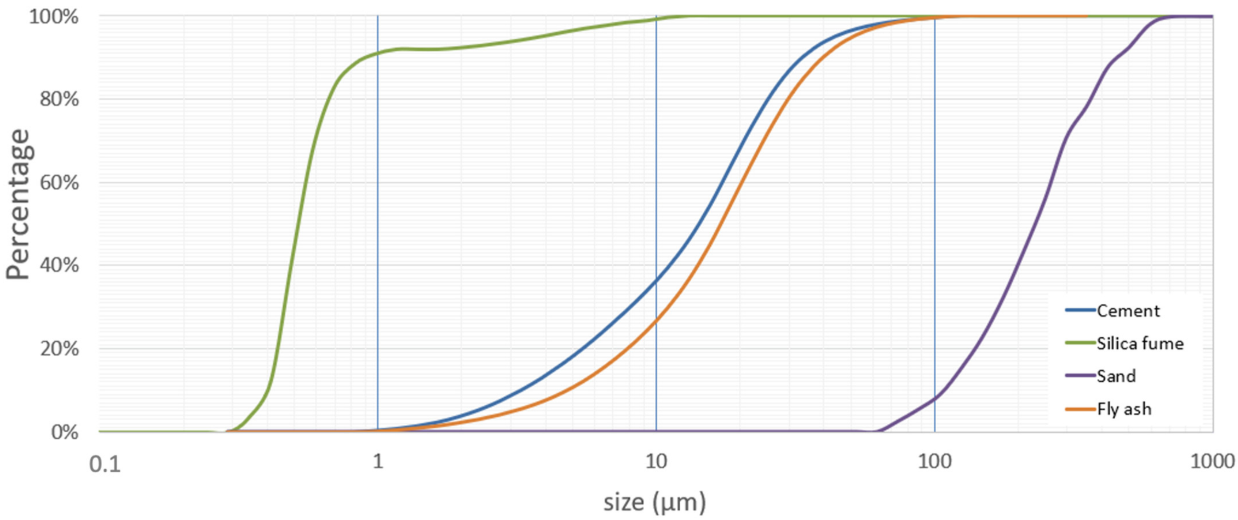

Figure 1. Granulometric distributions of UHPC materials.

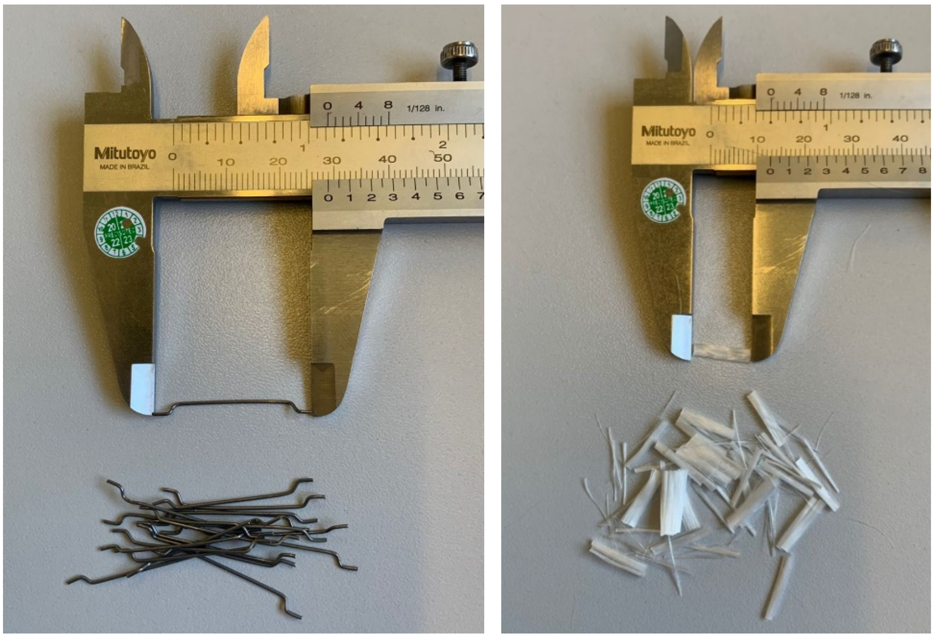

Figure 2. Steel and PVA fibers added to the UHPC.

To increase the flowability of the composite, the superplasticizer additive was used, without the need to add water.

The methodology consisted of two parts. The first part evaluated the variations (loss) in the compressive strength and modulus of elasticity by conducting compressive testing on cylinders of 100 mm in diameter and 200 mm in height according to ASTM C39 and ASTM C469, respectively. Four specimens were evaluated for each temperature and for each mechanical property tested, thus requiring a total of 40 specimens. The test specimens were subjected to the heating regime prescribed by standard ISO 834-1 up to a temperature of 400 °C. Higher temperatures were not considered due to the amount of spalling that occurred beyond this limit. The second part consisted of subjecting two columns with a cross-section of 250 mm × 250 mm and a height of 2800 mm to the heating regime of standard ISO 834-1 but not uniformly along all faces. Figure 3 shows the exposure of the faces of the columns and the oven used. Column dimensions have been defined to match actual element values. This simulated a real wall with masonry filling the gap between columns. The samples, after curing for 28 days, remained stored internally in the laboratory until the day of the test, in a condition of ambient temperature and humidity.

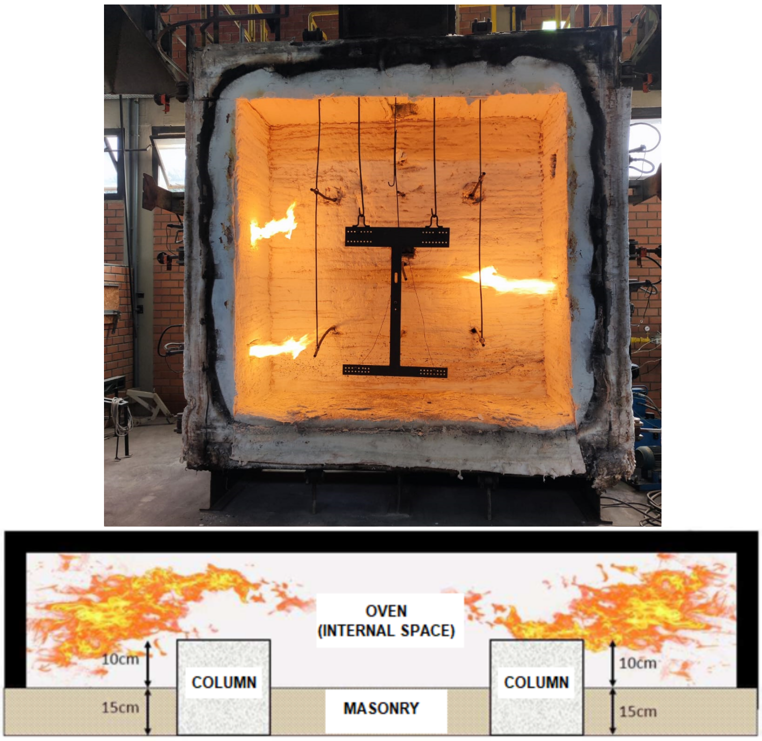

Figure 3. Top view of the column and masonry test in the kiln and the kiln used to carry out the test.

The columns and simulated wall were placed in a standard test frame with internal dimensions of 315 mm × 300 mm as shown in Figure 4. Masonry was coated with a layer of 10 mm-thick coarse plaster on the face exposed to heat.

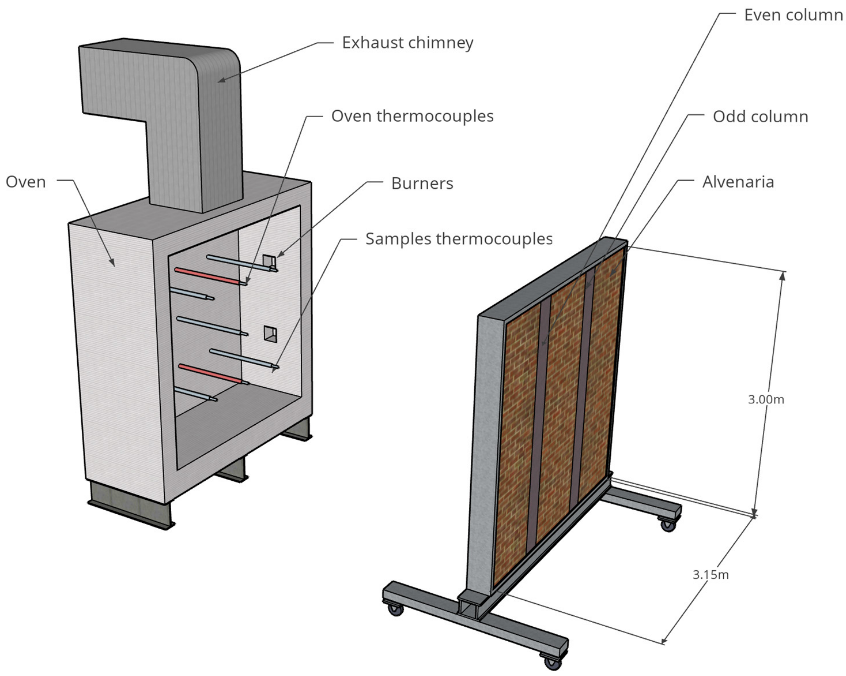

Figure 4. Placement of columns in the test frame and simulated wall and oven.

A protective screen was installed on the external face of the wall, as seen in Figure 5, as a safety measure against explosive spalling.

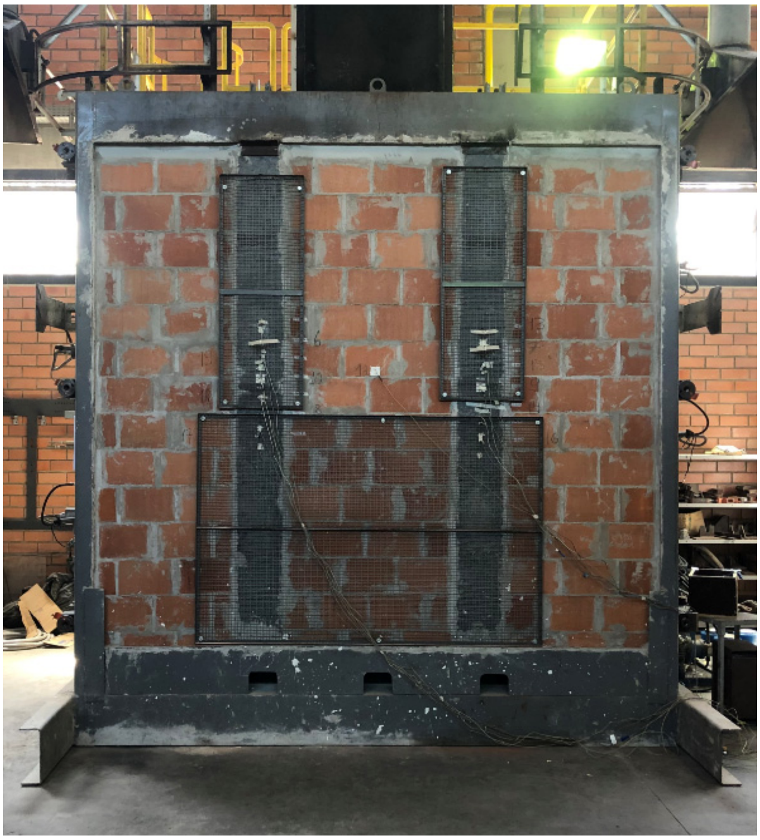

Figure 5. Protective screen on the external face of the wall.

Each column was equipped with seven T-type thermocouples on the geometric center of the face at different heights. This allowed for the measurements of temperatures along the cross-section. The depths and locations of the thermocouples are shown in Figure 6.

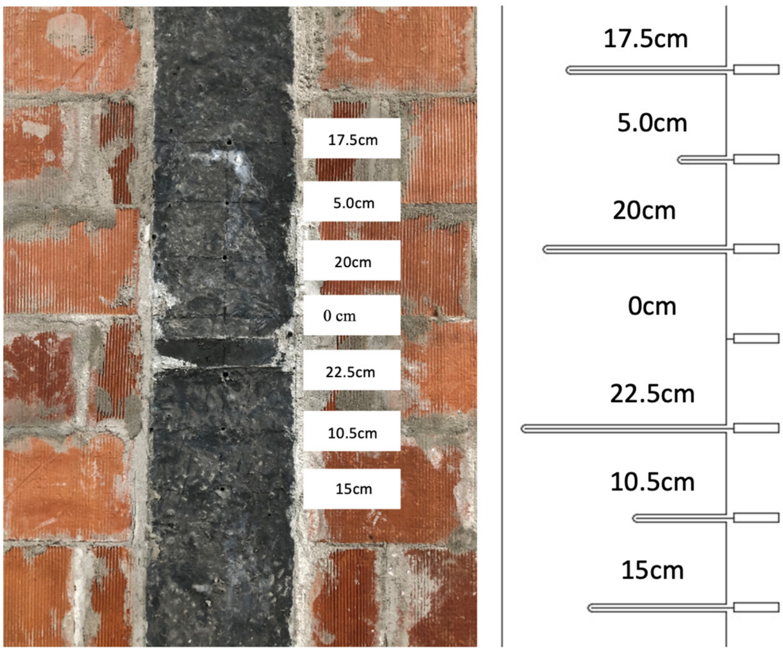

Figure 6. Locations and depths of thermocouples inserted in the columns.

The decrease in the cross-section was measured after the heating tests. This measurement was conducted by dividing the column into 12 sections along the height, as seen in Figure 7. Within each section, the decreases in the cross-section were measured at five locations, and five measurements were taken and averaged at each location.

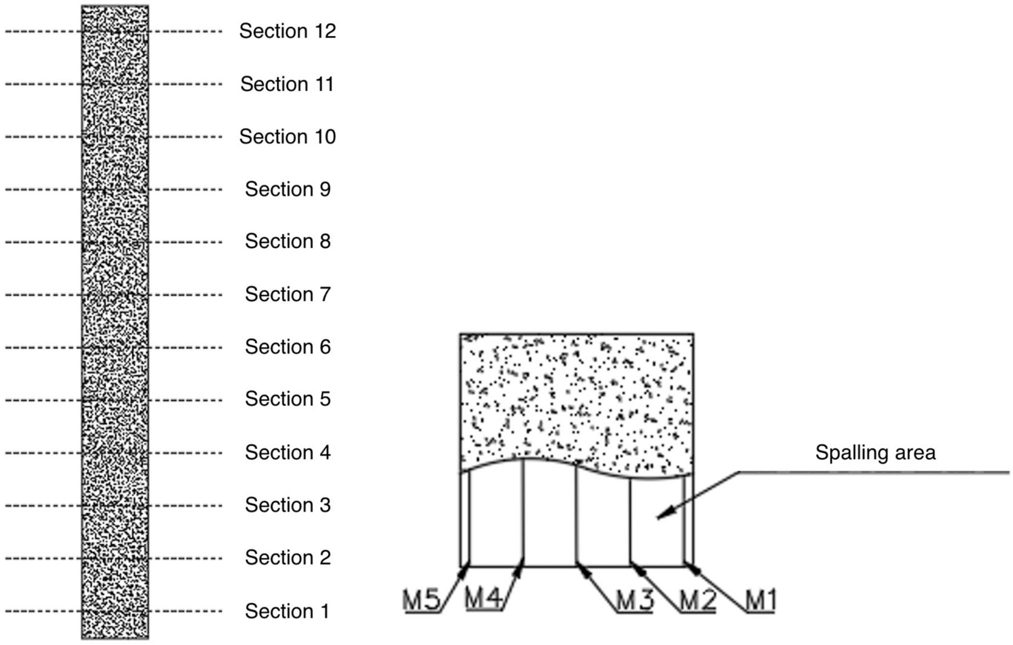

Figure 7. Locations of measurements of decreases in the cross-section.

3. Results

3.1. Losses of the Compressive Strength and Modulus of Elasticity Due to Exposure to High Temperatures

The values of the compressive strength and modulus of elasticity of the cylindrical specimens in relation to temperatures are shown in Figure 8.

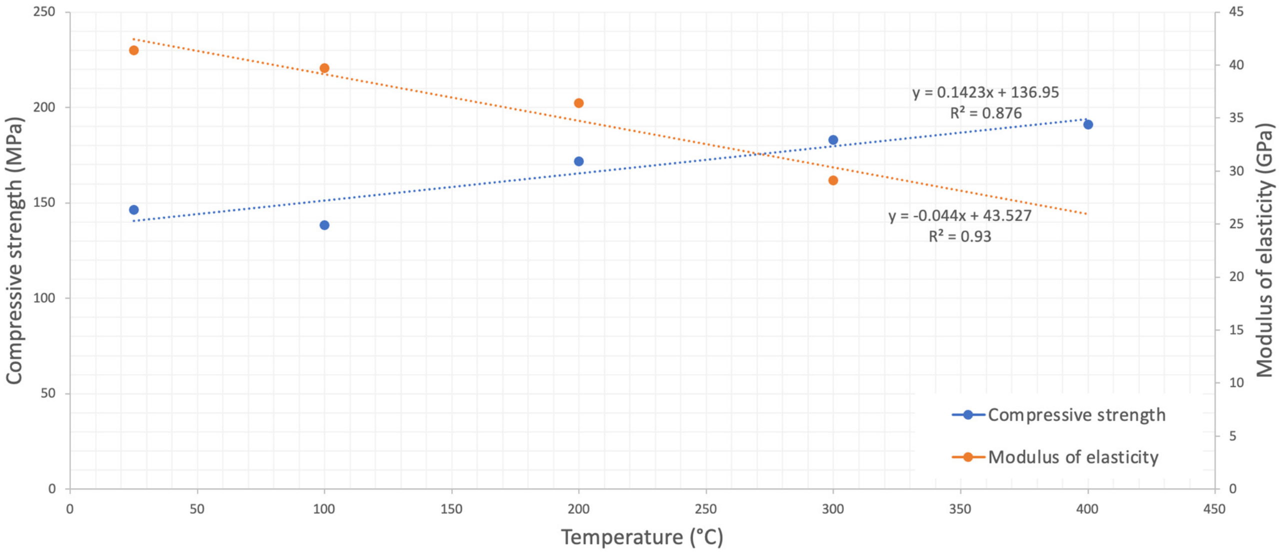

Figure 8. Variations in the compressive strength and modulus of elasticity with respect to temperature.

The mechanical properties of UHPC presented opposing trends concerning heating. The compressive strength increased with the increasing temperature up to a gain of 30.5% at 400 °C for the initial reference value. This increase in the compressive strength was also noted in other studies, such as Lee et al. [28], Xiong and Liew [13], and Morales et al. [29]. It is worth pointing out that this increase was only measured up to 400 °C due to the spalling of the UHPC at higher temperatures.

According to Peng et al. [30], the increase in the compressive strength was related to the hydration process of anhydrous cement and the chemical bonds between calcium hydroxide and pozzolans in the mixture. As the temperature increases, the strength of the concrete decreases. This loss is associated with the dehydration of the compounds and the decomposition of the formed crystals. However, at high temperatures, a rehydration process could occur due to the high pressure of intrinsic water, i.e., as compounds were dehydrated, water was adsorbed and could become available to form new compounds due to the presence of anhydrous cement [31]. This complex dehydration process contained phases of hydrated, partially hydrated, and dehydrated compounds. Each phase could be affected by the exposure temperature initial water/agglomerate ratio.

On the other hand, the modulus of elasticity presented a significant loss with the increasing temperature. At 300 °C, a decrease of 30% in the modulus of elasticity was registered for the initial reference value. This decrease could be related to the micro-fissuring of cement due to high temperatures, which would allow for more significant deformation associated with a reduction in the modulus of elasticity. Changes to the density due to high temperatures were also noted with decreases above 100 °C. There was a maximum decrease of 6% measured at 400 °C. Similar results were observed by Sanchayan and Foster [18] and Zheng and Wang [20].

3.2. Behaviors of Columns Exposed to Elevated Temperatures

Along the heating tests, several audible cracks were heard, resulting from spalling. The first cracks were noted in the first 5 min of testing and progressed in succession in intervals of approximately 5 min.

The spalling measurements are presented in Table 2, with the average decreases in the cross-section of columns 1 and 2 at the end of testing, which corresponded to 78 min.

Table 2. Losses of the cross-section and spalling of columns 1 and 2 at the end of testing.

	COLUMN 1		COLUMN 2	
Section	**Ave (mm)**	**Spalling**	**Ave (mm)**	**Spalling**
1	66.8	27%	57.2	23%
2	179.6	72%	61.6	25%
3	184.0	74%	104.0	42%
4	134.6	54%	122.0	49%
5	130.0	52%	46.8	19%
6	122.8	49%	135.4	54%
7	158.2	63%	154.2	62%
8	91.2	36%	165.0	66%
9	62.2	25%	134.2	54%
10	126.2	50%	120.4	48%
11	129.0	52%	114.6	46%
12	81.6	33%	93.0	37%
Average spalling		49%	Average spalling	44%

It is important to highlight that the concrete spalling did not occur in a single moment, but the spalling occurred gradually throughout the entire test. Cracks were heard, thus identifying the moment of the spalling occurrence. As shown in Table 2, spalling was not uniform. Spalling in column 1 varied between 25% and 74%, while in column 2, it varied between 19% and 66%. For a further comparison, Figure 9 graphically presents spalling in columns 1 and 2. No trend is apparent in Figure 9, but the most significant difference between columns 1 and 2 occurred in Section 2, near the base of the columns.

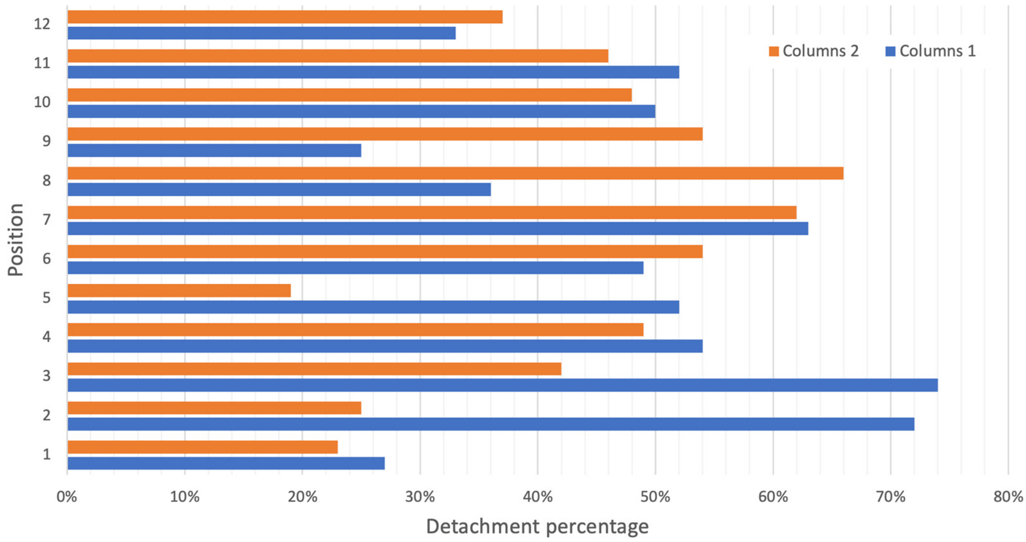

Figure 9. Spalling of columns 1 and 2 after exposure to elevated temperatures.

Figures 10 and 11 present the images of the spalling on columns 1 and 2, respectively.

(**a**) (**b**) (**c**) (**d**)

Figure 10. Column 1 after exposure to elevated temperatures: (**a**) whole column; (**b**) top 1/3 detail; (**c**) central 1/3 detail; (**d**) bottom 1/3 detail.

(a) (b) (c) (d)

Figure 11. Column 2 after exposure to elevated temperatures: (**a**) whole column; (**b**) top 1/3 detail; (**c**) central 1/3 detail; (**d**) lower 1/3 detail.

Figure 10 shows the non-uniformity of spalling of column 1. The central 1/3 portion (c) presented total spalling while the bottom 1/3 (d) was unaffected. Fibers could be observed in all spalling occurrences, which attested to the efficient dispersal of fibers in the UHPC.

Figure 11 shows that spalling in column 2 occurred mostly in the central 1/3 and top 1/3. Spalling behaviors were observed by Kahanji et al. [32] in the UHPC beams subjected to similar heating regimes but with concrete with a compressive strength of 131 MPa and a 2% steel fiber content. Similar to the results of this study, extensive spalling was observed along the entire length of the sample with variations in depth.

The high occurrence of spalling in the UHPC of this study was likely the result of a quartz sand aggregate in the mixture. As noted by Bulletin FIB 38 [14], quartz suffers from significant physical changes from thermal expansion when exposed to temperatures close to 500 °C. Further effects could be considered from the oxidation of metallic fibers and their thermal expansion, further decreasing adhesiveness to the matrix. These phenomena could have promoted deagglomeration, even though Zhang et al. [33] considered them to be inhibitors of spalling.

The heating curve applied in this study provided exposure to elevated temperatures in a short period, i.e., temperatures reached 600 °C in approximately 5 min, which would significantly affect the volume of the grains of quartz. The progressive spalling observed resulted from the low thermal conductivity of concrete. Spalling occurred in concrete constantly exposed to elevated temperatures sufficient to reach the critical expansion temperature of quartz. Figure 12 shows the temperature in columns 1 and 2 at several depths.

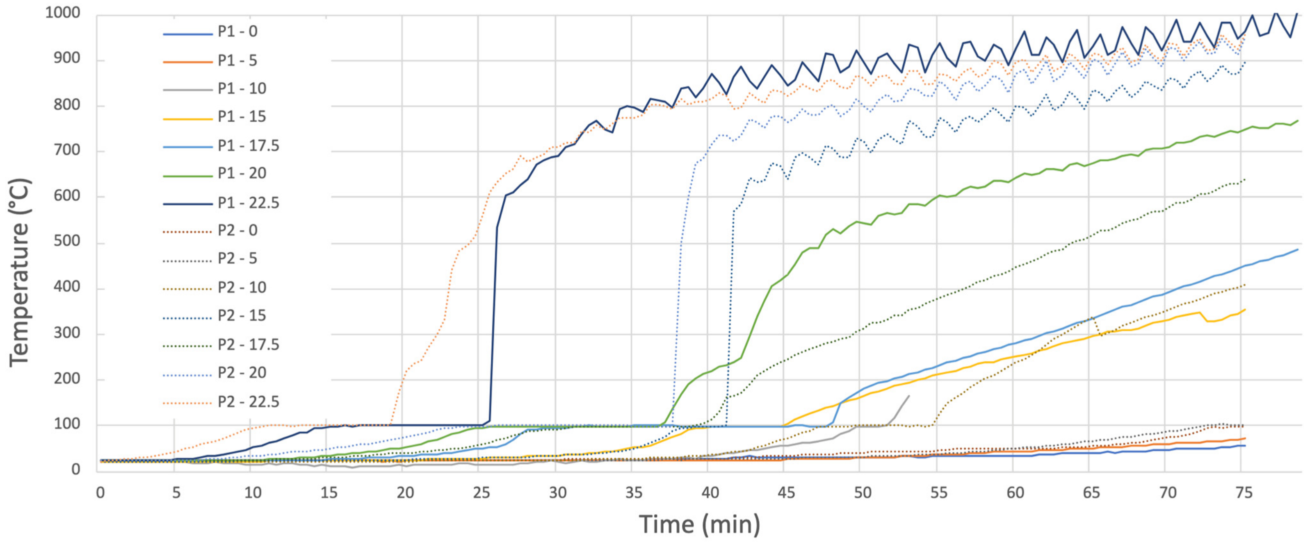

Figure 12. Temperatures at varying depths of column 1 and 2 over time.

As expected, Figure 12 shows that temperatures were lower deeper in the concrete. Stable plateaus were apparent at 100 °C at locations where spalling did not occur despite the exposure of the face of the concrete to high temperatures. These plateaus were due to water evaporation, which stabilized the temperature until the water was no longer present. This was in agreement with Mehta and Monteiro [34], who observed that the temperature only exceeded 100 °C after all free water had evaporated.

4. Conclusions

This study evaluated the behaviors of columns exposed to elevated temperatures. The main contribution of this paper was to measure the spalling on a real scale, which behaved differently than that in small samples. The columns evaluated were tested and reinforced only with fibers, and even considering this melting temperature, the mechanism that leads to spalling was extreme. Also, this paper showed the following results and conclusions:

- Comparing the results obtained with those reported in the bibliography, it should be mentioned that the high strength of the UHPC may lead to a higher displacement and spalling than in conventional concretes, even considering the lower water/cement ratios.
- UHPC exposed to elevated temperatures suffered from external degradation, which gradually changed the cross-section of the columns due to spalling.
- Up to a temperature of 400 °C, the compressive strength increased by up to 30.5% concerning the reference value. On the other hand, the modulus of elasticity and density decreased for the reference values, with peak reductions of 30% and 6%, respectively.
- The test results pointed out that the quartz sand aggregate in the mixture was deleterious to concrete performance and induced spalling as temperatures reached approximately 600 °C.
- The loss of the concrete session did not occur immediately, and there was a progressive detachment of the concrete due to heating. Once a heated piece of concrete was loosened, a new surface was exposed and again, it was heated to the point of spalling. This phenomenon caused small cracks that were possible to hear during the tests.

Author Contributions: Conceptualization, R.C., H.Z.E., F.P. and A.M.G.; methodology, L.R.L., G.P., R.C., H.Z.E., F.P. and F.L.B.; validation, B.F.T. All authors have read and agreed to the published version of the manuscript.

Funding: This research received no external funding.

Data Availability Statement: Not applicable.

Acknowledgments: The authors are grateful for the assistance in carrying out the tests and purchasing raw materials, especially by its Performance—UNISINOS.

Conflicts of Interest: The authors declare no conflict of interest.

References

1. Christ, R. *Proposição de um Método de Dosagem Para Concretos de Ultra Alto Desempenho (UHPC)*; Universidade do Vale do Rio dos Sinos: Unisinos, Brazil, 2019.
2. Torregrosa, E.C. Dosage Optimization and Bolted Connections for UHPFRC Ties. Ph.D. Thesis, Universidad Politécnica de Valencia (UPV), Valencia, Spain, 2013.
3. ACI. *ACI Committee 239 Ultra-High Performance Concrete 2012 ACI Fall Convention*; ACI Fall Convention: Toronto, ON, Canada, 2013; pp. 5–8.
4. *NF P18-470*; Concrete—Ultra-High Performance Fibre-Reinforced Concrrte—Specifications, Performance, Production and Conformity. Association Française de Normalisation: La Plaine Saint-Denis, France, 2016; 94p.
5. Perry, V.; Alberta, C.; Guilherme, A.P. *Nova Fronteira Para o Concreto*; Revista Estrutura: São Paulo, Brazil, 2019; pp. 25–33.
6. Christ, R.; Tutikian, B. Study of pressure and curing temperature in reactive powder concretes (RPC) with different amounts of metallic microfibers. *Rev. La Constr.* **2013**, *12*, 30–38. [CrossRef]
7. Resplendino, J. Ultra high performance concrete: New AFGC recommendations. In *Designing and Building with UHPFRC*; John Wiley & Sons, Inc.: Hoboken, NJ, USA, 2013; pp. 713–722. [CrossRef]
8. Fehling, E.; Schmidt, M.; Walraven, J.; Leutbecher, T.; Frihlich, S. *Ultra-High Performance Concrete UHPC: Fundamentals, Design, Examples*; Wilhelm Ernst & Sohn: Hoboken, NJ, USA, 2015. [CrossRef]
9. Bolina, F.L. Avaliação Experimental da Influência dos Requisitos de Durabilidade na Segurança Contra Incêndio de Protóptipos de Pilares Pré-Fabricados de Concreto Armado. Master's Thesis, Universidade do Vale do Rio dos Sinos (UNISINOS), São Leopoldo, Brazil, 2016; 170p.
10. Hennemann, G.G.; Gil, A.M.; Fernandes, B.; Bolina, F.L.; Tutikian, B.F. Avaliação teórico-experimental da influência da espessura de alvenaria na resistência ao fogo de sistemas verticais de vedação. *Ambient. Const.* **2017**, *17*, 183–195. [CrossRef]
11. Kodur, V. *Properties of Concrete at Elevated Temperatures*; Hindawi Publishing Corporation: London, UK, 2014; pp. 1–15. [CrossRef]
12. Xiong, M.X.; Liew, J.Y.R. Spalling behavior and residual resistance of fibre reinforced Ultra-High performance concrete after exposure to high temperatures. *Mater. Constr.* **2015**, *65*, 2–10. [CrossRef]
13. Gil, A.; Pacheco, F.; Christ, R.; Bolina, F.; Khayat, K.H.; Tutikian, B. Comparative study of concrete panels' fire resistance. *ACI Mater. J.* **2017**, *114*, 2017. [CrossRef]
14. FIB. *FIB 38—Fire Design of Concrete Structures*; Fédération Internationale du Béton (FIB): Lausanne, Switzerland, 2008; Volume 38, p. 106. [CrossRef]
15. Li, Y.; Tan, K.H.; Yang, E.H. Synergistic effects of hybrid polypropylene and steel fibers on explosive spalling prevention of ultra-high performance concrete at elevated temperature. *Cem. Concr. Compos.* **2018**, *96*, 174–181. [CrossRef]
16. Zhang, D.; Dasari, A.; Hai, K. On the mechanism of prevention of explosive spalling in ultra-high performance concrete with polymer fibers. *Cem. Concr. Res.* **2018**, *113*, 169–177. [CrossRef]
17. Dias, D.M.; Calmon, J.L.; Vieira, G.L. Polymeric fiber reinforced concrete exposed to fire. *Rev. ALCONPAT* **2020**, *10*, 36–52. [CrossRef]
18. Sanchayan, S.; Foster, S.J. High temperature behaviour of hybrid steel–PVA fibre reinforced reactive powder concrete. *Mater. Struct. Mater. Constr.* **2016**, *49*, 769–782. [CrossRef]
19. Choe, G.; Kim, G.; Gucunski, N.; Lee, S. Evaluation of the mechanical properties of 200 MPa ultra-high-strength concrete at elevated temperatures and residual strength of column. *Constr. Build. Mater.* **2015**, *86*, 159–168. [CrossRef]
20. Zheng, W.; Wang, Y. Microstructure and mechanical properties of RPC containing PP fibres at elevated temperatures. *Mag. Concr. Res.* **2014**, *66*, 397–408. [CrossRef]
21. Li, Y.; Pimienta, P.; Pinoteau, N.; Tan, K.H. Effect of aggregate size and inclusion of polypropylene and steel fibers on explosive spalling and pore pressure in ultra-high-performance concrete (UHPC) at elevated temperature. *Cem. Concr. Compos.* **2019**, *99*, 62–71. [CrossRef]
22. Gravit, M.; Golub, E. Increase of fire resistance of reinforced concrete structures with polypropylene microfiber. In *MATEC Web of Conferences*; EDP Sciences: Yulis, France, 2018. [CrossRef]
23. Adesina, A. Overview of the in fl uence of waste materials on the thermal conductivity of cementitious composites. *Clean Eng. Technol.* **2020**, *2*, 100046. [CrossRef]
24. Abid, M.; Hou, X.; Zheng, W.; Hussain, R.R. High temperature and residual properties of reactive powder concrete—A review. *Constr. Build. Mater.* **2017**, *147*, 339–351. [CrossRef]
25. Kodur, V.K.R.; Cheng, F.-P.; Wang, T.-C.; Sultan, M.A. Effect of strength and fiber reinforcement on fire resistance of high-strength concrete columns. *J. Struct. Eng.* **2003**, *129*, 253–259. [CrossRef]
26. Bolina, F.L.; Gil, A.M.; Fernandes, B.; Hennemann, G.G.; Goncalves, J.; Tutikian, B.F. Influence of design durability on concrete columns fire performance. *J. Mater. Res. Technol.* **2020**, *9*, 4968–4977. [CrossRef]

27. Manica, G.C.; Bolina, F.L.; Tutikian, B.F.; Oliveira, M.; Moreira, M.A. Influence of curing time on the fire performance of solid reinforced concrete plates. *J. Mater. Res. Technol.* **2020**, *9*, 2506–2512. [CrossRef]
28. Lee, N.K.; Koh, K.T.; Park, S.H.; Ryu, G.S. Microstructural investigation of calcium aluminate cement-based ultra-high performance concrete (UHPC) exposed to high temperatures. *Cem. Concr. Res.* **2017**, *102*, 109–118. [CrossRef]
29. Morales, D.S.; Ríos, J.D.; La Concha, A.M.D.; Cifuentes, H.; Jiménez, J.R.; Fernández, J.M. Effect of moderate temperatures on compressive strength of ultra-high performance concrete: A microstructurak analysis. *Cem. Concr. Res.* **2021**, *140*, 19. [CrossRef]
30. Peng, G.F.; Chan, S.Y.N.; Anson, M. Chemical kinetics of C-S-H decomposition in hardened cement paste subjected to elevated temperatures up to 800 °C. *Adv. Cem. Res.* **2001**, *13*, 47–52. [CrossRef]
31. Xuan, D.X.; Shui, Z.H. Rehydration activity of hydrated cement paste exposed to high temperature. *Fire Mater.* **2011**, *35*, 481–490. [CrossRef]
32. Kahanji, C.; Ali, F.; Nadjai, A. Experimental study of ultra-high performance fibre reinforced concrete under ISO 834 fire. In *Proceeding of the Ninth International Conference on Structures in Fire, Princeton, NJ, USA, 8–10 June 2016*; DEStech Publications, Inc.: Lancaster, PA, USA, 2016; Volume 165. [CrossRef]
33. Zhang, Y.; Wei, Y.; Bai, J.; Wu, G.; Dong, Z. A novel seawater and sea sand concrete filled FRP-carbon steel composite tube column: Concept and behaviour. *Compos. Struct.* **2020**, *246*, 13. [CrossRef]
34. Mehta, P.K.; Monteiro, P.J. Concreto microestrutura, propriedades e materiais. In *Ibracon*, 4th ed.; Ibracon: São Paulo, Brazil, 2014.